Determination of Carbide, Carbyne, and Carbene Bond Energies by Gas-Phase Photodissociation of $RhCH_2^+$, $NbCH_2^+$, and $LaCH_2^+$

R. L. Hettich and B. S. Freiser*

Contribution from the Department of Chemistry, Purdue University, West Lafayette, Indiana 47907. *Received June 11, 1986*

Abstract: Three photoproducts, MCH^+, MC^+, and M^+, are observed in the photodissociation of MCH_2^+ (M = Rh, Nb, and La). In contrast, the low-energy collision-induced dissociation of $RhCH_2^+$ and $NbCH_2^+$ yields MC^+ and M^+ whereas $LaCH_2^+$ produces only La^+. Each photodissociation spectrum reveals two peaks: 240 nm (σ = 0.06 Å^2) and 280 nm for $RhCH_2^+$, 240 nm (σ = 0.20 Å^2) and 390 nm for $NbCH_2^+$, and 260 nm (σ = 0.19 Å^2) and 320 nm for $LaCH_2^+$. Photoappearance thresholds for the products yield bond energies for M^+–CH_2, M^+–CH, and M^+–C for each metal ion. Ionization potentials for RhC, NbC, and LaC are calculated on the basis of $D°(M–C)$ and $D°(M^+–C)$. Plots of metal–ion ligand bond energies vs. bond energies for corresponding carbon analogues show linear correlation and allow bond order predictions to be made for the metal complexes.

One of the primary goals of gas-phase organometallic chemistry is to investigate the fundamental bonding and energetics of transition metal–ligand ions in solvent-free conditions. Photodissociation is one method that appears to provide this information, complementing other theoretical[1] and experimental[2] techniques.

The photodissociation spectrum of an ion is obtained by monitoring the disappearance of the ion (or by monitoring the appearance of photoproducts) as a function of wavelength, reaction 1. Preliminary studies have indicated that photodissociation can

$$AB^+ + h\nu \rightarrow \begin{cases} A^+ + B \\ B^+ + A \end{cases} \quad (1)$$

provide both thermodynamic and spectroscopic information for organometallic ions.[3]

In an earlier report investigating the bond energies of $FeCH_2^+$ and $CoCH_2^+$ by photodissociation, we observed three photofragments, reactions 2–4 in contrast to the collision-induced

$$MCH_2^+ + h\nu \rightarrow \begin{cases} M^+ + CH_2 & (2) \\ MC^+ + H_2 & (3) \\ MCH^+ + H & (4) \end{cases}$$

dissociation, which gave M^+ as the only fragment.[4] Observation of the photoappearance onsets provided a method of obtaining thermochemical information for MCH_2^+, MCH^+, and MC^+. The interest in metal–alkyl, metal–alkylidene, and metal–alkylidyne stems from the possible role that these species may have as intermediates in both homogeneous and heterogeneous reactions (e.g., Fischer–Tropsch synthesis of hydrocarbons, olefin metathesis, Ziegler–Natta polymerization of olefins).[5] Various theoretical[6] as well as experimental[7] studies have focused on these types of complexes.

This report examines the photodissociation of $RhCH_2^+$, $NbCH_2^+$, and $LaCH_2^+$ in an effort to investigate the corresponding carbenes, carbynes, and carbides. These ions were chosen because they can be conveniently generated in the gas phase and should indicate how transition metal–ion bonding to CH_n (n = 0–2) groups varies as the electron density and the size of the metal ion varies.

Experimental Section

All experiments were performed on a prototype Nicolet FTMS-1000 Fourier transform mass spectrometer equipped with laser ionization for generating metal ions.[8] The 5.2 cm cubic cell, which is situated between the poles of a Varian 15-in. electromagnet maintained at 0.85 T, utilized two 80% transmittance stainless steel screens as the transmitter plates in order to permit irradiation of the trapped ions. M^+ for M = Rh, Nb, La was generated by focusing the frequency-doubled line (532 nm) of a Nd:YAG laser onto the appropriate metal foil[9] and then reacted with a neutral reagent gas, as discussed below, to generate MCH_2^+. The neutral reagent gases were admitted to the cell via a pulsed valve[10] in order to eliminate interfering secondary reactions. Ion ejection was used to isolate the MCH_2^+ for the photodissociation experiments. This isolation step may in some cases leave the MCH_2^+ with some excess kinetic energy. A static argon pressure of $\sim 2 \times 10^{-6}$ Torr was used in each experiment to collisionally cool the ions prior to dissociation. Insufficient cooling of the ions would result in bond energy values that are too low. The ions were trapped for 3–7 s (depending on the cross section for photodissociation) while being irradiated with light from a 2.5 kW Hg–Xe arc lamp used in conjunction with a 0.25-m Schoeffel monochromator set for 10-nm resolution.

The concentration of the ions in the cell at $\sim 10^{-18}$ M precluded monitoring the absorption spectrum directly; hence, ionic photoproducts were monitored as a function of wavelength. Poor reproducibility of the laser ionization pulse (shot-to-shot variation) made monitoring the disappearance of the parent ions impractical. Because of this, the ratio of ion photoproduct intensities to parent ion intensity was monitored as a function of wavelength. Cutoff filters were also used to identify thresholds. A spectroscopic threshold will yield only upper limits for bond energies. However, preliminary studies have suggested that for these metal ion–ligand systems, the thresholds yield absolute bond energy information.[3]

(1) (a) Alvarado-Swaisgood, A. E.; Harrison, J. F. *J. Phys. Chem.* **1985**, *89*, 5198. (b) Ross, R. B.; Ermler, W. C. *J. Phys. Chem.* **1985**, *89*, 5202. (c) Schilling, J. B.; Goddard, W. A., III; Beauchamp, J. L. *J. Am. Chem. Soc.* **1986**, *108*, 582. (d) Krauss, M.; Stevens, W. J. *J. Chem. Phys.* **1985**, *82*, 5584.

(2) (a) Houriet, R.; Halle, L. F.; Beauchamp, J. L. *Organometallics* **1983**, *2*, 1818. (b) Armentrout, P. B.; Loh, S. K.; Ervin, K. M. *J. Am. Chem. Soc.* **1984**, *106*, 1161. (c) Jacobson, D. B.; Freiser, B. S. *J. Am. Chem. Soc.* **1985**, *107*, 1581. (d) Wronka, J.; Ridge, D. P. *J. Am. Chem. Soc.* **1984**, *106*, 67. (e) Bondybey, V. E. *Science* **1985**, *227*, 125. (f) Smalley, R. E. *Laser Chem.* **1983**, *2*, 167. (g) Leopold, D. G.; Miller, T. M.; Lineberger, W. C. *J. Am. Chem. Soc.* **1986**, *108*, 178.

(3) (a) Cassady, C. J.; Freiser, B. S. *J. Am. Chem. Soc.* **1984**, *106*, 6176. (b) Hettich, R. L.; Jackson, T. C.; Stanko, E. M.; Freiser, B. S. *J. Am. Chem. Soc.* **1986**, *108*, 5086.

(4) Hettich, R. L.; Freiser, B. S. *J. Am. Chem. Soc.* **1986**, *108*, 2537.

(5) (a) Fischer, E. O. *Adv. Organomet. Chem.* **1976**, *14*, 1. (b) Fischer, E. O.; Schubert, U.; Fischer, H. *Pure Appl. Chem.* **1978**, *50*, 857.

(6) (a) Alvarado-Swaisgood, A. E.; Allison, J.; Harrison, J. F. *J. Phys. Chem.* **1985**, *89*, 2517. (b) Carter, E. A.; Goddard, W. A., III *J. Phys. Chem.* **1984**, *88*, 1485. (c) Shim, I.; Gingerich, K. A. *J. Chem. Phys.* **1982**, *76*, 3833. (d) Ushio, J.; Nakatsuji, H.; Yonezawa, T. *J. Am. Chem. Soc.* **1984**, *106*, 5892. (e) Mavidis, A.; Alvarado-Swaisgood, A. E.; Harrison, J. F. *J. Phys. Chem.* **1986**, *90*, 2584. (f) Carter, A. E.; Goddard, W. A., III *J. Am. Chem. Soc.* **1986**, *108*, 2180.

(7) (a) Pelino, M.; Gingerich, K. A.; Haque, R.; Kingcade, J. E. *J. Phys. Chem.* **1985**, *89*, 4257. (b) Pelino, M.; Gingerich, K. A.; Nappi, B.; Haque, R. *J. Chem. Phys.* **1984**, *80*, 4478. (c) Stevens, A. E.; Beauchamp, J. L. *J. Am. Chem. Soc.* **1979**, *101*, 6449. (d) Jacobson, D. B.; Freiser, B. S. *J. Am. Chem. Soc.* **1985**, *107*, 2605.

(8) Burnier, R. C.; Cody, R. B.; Freiser, B. S. *Anal. Chem.* **1982**, *54*, 96.

(9) Burnier, R. C.; Byrd, G. D.; Carlin, T. J.; Wise, M. B.; Cody, R. B.; Freiser, B. S. *Lecture Notes in Chemistry*; Wanczek, K. P., Ed.; Springer-Verlag: West Germany, 1982.

(10) Carlin, T. J.; Freiser, B. S. *Anal. Chem.* **1983**, *55*, 571.

0002-7863/87/1509-3543$01.50/0

To obtain absolute values for the cross sections of the ions being examined, the photodissociation of $C_7H_8^+$ (from toluene at 20 eV) at 410 nm (σ = 0.05 Å^2)[11] was compared to the photodissociation of a given ion at its λ_{max}, both taken under similar experimental conditions. All cross sections determined in this manner have an estimated uncertainty of ±50% due to instrumental variables.

Results and Discussion

$RhCH_2^+$. Rh^+ will react with either cyclopropane or ethylene oxide to abstract carbene, reactions 5 and 6.[12] Reaction 5 indicates that $D°(Rh^+–CH_2) \geq 93$ kcal/mol; observation of reaction 6 implies $D°(Rh^+–CH_2) \geq 78$ kcal/mol.[13] Reaction 6 is more rapid than reaction 5 and, therefore, was used to generate $RhCH_2^+$ for the photodissociation experiment. Reaction 7 has been reported, placing an upper limit of 96 kcal/mol for $D°(Rh^+–CH_2)$ and suggesting $D°(Rh^+–CH_2) = 94 \pm 5$ kcal/mol.[12b]

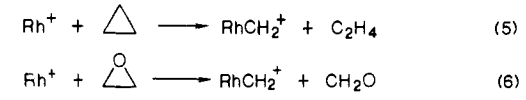

$$RhCH_2^+ + CH_4 \rightarrow Rh^+ + C_2H_6 \quad (7)$$

Photodissociation of $RhCH_2^+$ yields all three products, reactions 2–4, with Rh^+ as the major photoproduct at most wavelengths. Only a small amount of $RhCH^+$ is observed. Collision-induced dissociation (CID) of $RhCH_2^+$ results in both dehydrogenation and carbene elimination to generate RhC^+ and Rh^+, respectively, with Rh^+ as the major product,[12b] and in this sense it is virtually indistinguishable from photodissociation. Figure 1a illustrates the overall photoappearance spectrum combining all three photoproducts (this spectrum should be equivalent to the photodissociation spectrum for $RhCH_2^+$); the photoappearance spectra for the ions of reactions 2–4 are shown in Figure 1b,c. Figure 1a reveals a major peak at 240 nm (σ = 0.06 Å^2).

Figure 1b indicates a photoappearance onset for Rh^+ at 320 nm, implying $D°(Rh^+–CH_2) = 89 \pm 5$ kcal/mol. This bond energy is ~5 kcal/mol lower than the value obtained by ion–molecule bracketing. Internal energy present in $RhCH_2^+$, resulting from reaction exothermicity or kinetic excitation during isolation, would move the threshold of Rh^+ to lower energies and could account for the discrepancy observed above. Two methods which should lower the amount of internal energy in the ion were utilized to investigate this effect: (1) generation of $RhCH_2^+$ by reaction 5 (less exothermic than reaction 6), and (2) increasing the static pressure of argon (to cool the ions once they are formed). $RhCH_2^+$ generated by reaction 5 photodissociates readily at 310 nm, implying $D°(Rh^+–CH_2) < 92$ kcal/mol. In addition, increased argon pressure also had no effect on dissociation at wavelengths less than 310 nm. On the basis of reaction 5, the photodissociation threshold of Rh^+, and the factors stated above, $D°(Rh^+–CH_2) = 91 \pm 5$ kcal/mol is assigned yielding $\Delta H_f°(RhCH_2^+) = 308 \pm 5$ kcal/mol.

Figure 1c shows the photoappearance spectra of $RhCH^+$ and RhC^+. The photoappearance onset for $RhCH^+$ is difficult to determine since it is a very minor photoproduct. $RhCH^+$, however, is readily observed at 300 nm, implying $D°(RhCH^+–H) < 95$ kcal/mol, and has a threshold near 320 nm, suggesting $D°(RhCH^+–H) = 89 \pm 5$ kcal/mol, $\Delta H_f°(RhCH^+) = 345 \pm 7$ kcal/mol, and $D°(Rh^+–CH) = 102 \pm 7$ kcal/mol,[13] in the same range as the results for Fe, Co, and V.[4,14] RhC^+ appears at wavelengths at least out to 600 nm, implying $D°(RhC^+–H_2) < 48$ kcal/mol, $\Delta H_f°(RhC^+) < 356$ kcal/mol, and $D°(Rh^+–C) > 120$ kcal/mol.[13] These values suggest $D°(RhC^+–H) < 63$ kcal/mol.

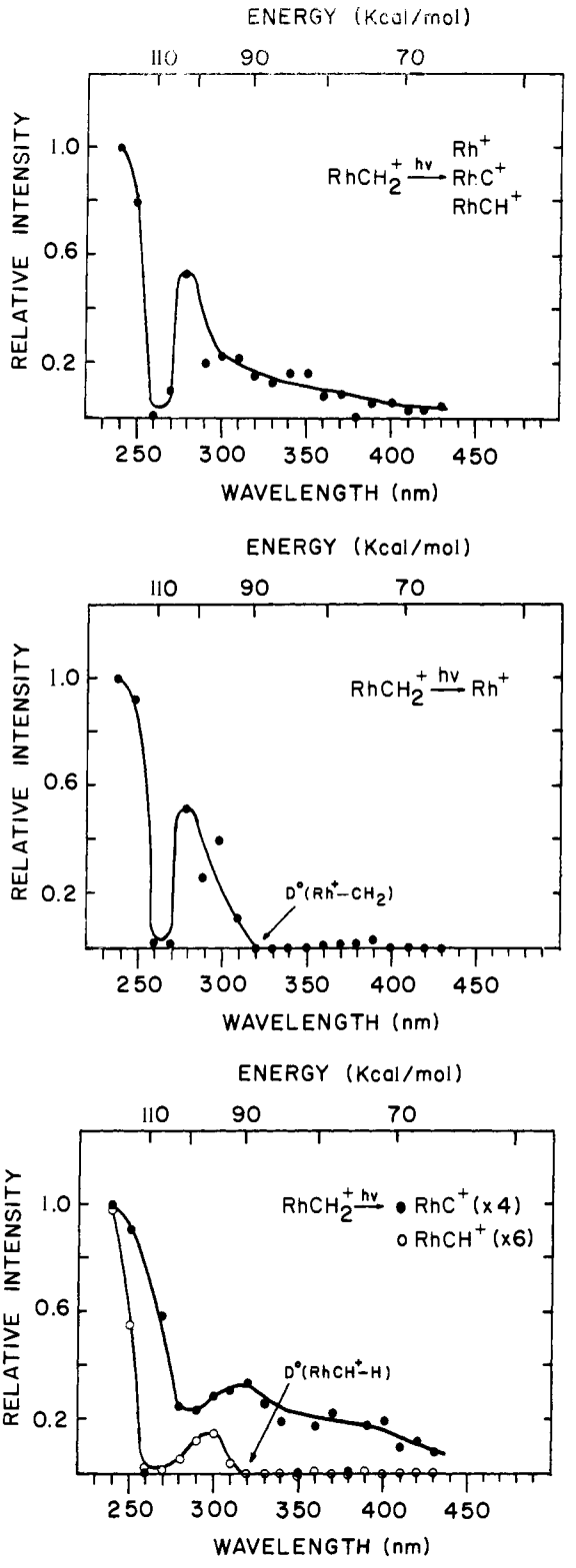

Figure 1. (a, top) The photodissociation spectrum of $RhCH_2^+$ obtained by monitoring all three photoproducts, reactions 2–4, as a function of wavelength. (b, middle) The photoappearance spectrum of Rh^+ obtained by monitoring reaction 2 as a function of wavelength. (c, bottom) The photoappearance spectra of $RhCH^+$ (open circles) and RhC^+ (closed circles) obtained by monitoring reactions 3 and 4 as a function of wavelength. The intensities of these two photoproducts have been scaled relative to the intensity of Rh^+ in spectrum b, which was assigned to be 1.0 at 240 nm.

RhC^+ can also be obtained by reacting Rh^+ with cycloheptatriene, reaction 8,[15] implying $D°(Rh^+–C) > 148$ kcal/mol. Rh^+ will not abstract carbide from toluene, possibly indicating $D°(Rh^+–C) < 179$ kcal/mol. The limits suggest $D°(Rh^+–C) =$

(11) Dunbar, R. C. *Chem. Phys. Lett.* **1975**, *32*, 508.
(12) (a) Byrd, G. D.; Freiser, B. S. *J. Am. Chem. Soc.* **1982**, *104*, 5944. (b) Jacobson, D. B.; Freiser, B. S. *J. Am. Chem. Soc.* **1985**, *107*, 5870.
(13) Heats of formation (and other thermochemical values) for all organic molecules, radicals, and metal ions are taken from the following: Rosenstock, H. M.; Draxl, K.; Steiner, B. W.; Herron, J. T. *J. Phys. Chem. Ref. Data, Suppl. 1* **1977**, *6*.
(14) Aristov, N.; Armentrout, P. B. *J. Am. Chem. Soc.* **1984**, *106*, 4065.

$$Rh^+ + \bigcirc \longrightarrow RhC^+ + (C_6H_6 + H_2) \quad (8)$$

164 ± 16 kcal/mol.[15] The photodissociation limit for $D°(Rh^+–C)$, while significantly lower, is consistent with this value. Table I summarizes the carbene, carbyne, and carbide bond energies for these ions as well as the values for iron and cobalt.

Ab initio HF–CI calculations on RhC indicate a triple bond and $D°(Rh–C)$ = 137.7 ± 0.9 kcal/mol has been determined mass spectrometrically.[16] The bond energies of RhC and RhC^+ ($D°(Rh^+–C)$ = 164 ± 16 kcal/mol[15]) suggest IP(RhC) = 6.4 ± 0.7 eV. Finally, the bond energy of RhC and $\Delta H_f°(RhCH^+)$ = 345 ± 7 kcal/mol determined from this study yield a proton affinity of RhC, PA(RhC) = 186 ± 8 kcal/mol.[13]

$LaCH_2^+$. La^+ will abstract carbene from both propene and cyclopropane, reactions 9 and 10, but is unreactive with methane.[17] Reaction 9 requires $D°(La^+–CH_2) \geq 101$ kcal/mol while reaction 10 implies $D°(La^+–CH_2) \geq 93$ kcal/mol.[13] Absence of reaction

$$La^+ + \diagup\!\!\diagdown \longrightarrow LaCH_2^+ + C_2H_4 \quad (9)$$

$$La^+ + \triangle \longrightarrow LaCH_2^+ + C_2H_4 \quad (10)$$

with methane might suggest $D°(La^+–CH_2) \leq 112$ kcal/mol. These results indicate $D°(La^+–CH_2)$ = 106 ± 5 kcal/mol. $LaCH_2^+$ does not react with either H_2 or CH_4 to produce La^+, so no upper limit for $D°(La^+–CH_2)$ could be obtained by these ion–molecule reactions. Collision-induced dissociation of $LaCH_2^+$ results in exclusive cleavage of CH_2 to form La^+.

Photodissociation of $LaCH_2^+$ yields La^+, LaC^+, and $LaCH^+$ (reactions 2–4), all in good abundance. LaO^+ is also observed, as a result of rapid secondary reactions of the three photoproducts with background oxygen, and must be monitored to account for the intensity of all the photoproducts. Two peaks are observed in Figure 2a, the photodissociation spectrum of $LaCH_2^+$, at 260 nm (σ = 0.19 Å^2) and 320 nm.

The threshold for La^+ observed at 270 nm, Figure 2b, implies $D°(La^+–CH_2)$ = 106 ± 5 kcal/mol and $\Delta H_f°(LaCH_2^+)$ = 219 ± 5 kcal/mol, in excellent agreement with the values obtained by ion–molecule reactions.

The photoappearance spectra of $LaCH^+$ and LaC^+, shown in Figure 2c, reveal not only the peak at 250 nm but an additional peak at ~300 nm. The photoappearance onset for $LaCH^+$ occurs at 350 nm, indicating $D°(LaCH^+–H)$ = 82 ± 7 kcal/mol. This value yields $\Delta H_f°(LaCH^+)$ = 249 ± 8 kcal/mol and $D°(La^+–CH)$ = 125 ± 8 kcal/mol. The photoappearance spectrum of LaC^+ reveals peak maxima at 250 nm and 320 nm with a threshold at 350 nm, suggesting $D°(LaC^+–H_2)$ = 82 ± 5 kcal/mol, $\Delta H_f°(LaC^+)$ = 301 ± 8 kcal/mol, and $D°(La^+–C)$ = 102 ± 8 kcal/mol.[13] Reaction of La^+ with cycloheptatriene produces $LaCH_2^+$, but LaC^+ is not observed, as expected since $D°(M^+–C)$ must exceed 148 kcal/mol to abstract carbide from cycloheptatriene. From the values given above, $D°(LaC^+–H)$ = 104 ± 11 kcal/mol is obtained, which is in accord with a C–H bond energy.

$D°(La–C)$ = 111 ± 8 kcal/mol has been estimated.[18] IP(LaC) = 6.0 ± 0.5 eV is inferred from this value and $D°(La^+–C)$ determined above. PA(LaC) = 279 ± 16 kcal/mol is derived from $D°(La–C)$ and $\Delta H_f°(LaCH^+)$.[13]

$NbCH_2^+$. Nb^+ is one of the few metal ions that will react with methane, reaction 11,[19] suggesting $D°(Nb^+–CH_2) \geq 112$ kcal/mol.

$$Nb^+ + CH_4 \rightarrow NbCH_2^+ + H_2 \quad (11)$$

$NbCH_2^+$ can be generated in better yield by reaction 12, which requires $D°(Nb^+–CH_2) \geq 93$ kcal/mol.[13] However, reaction 11

$$Nb^+ + \triangle \longrightarrow NbCH_2^+ + C_2H_4 \quad (12)$$

was used to generate the $NbCH_2^+$ for the photodissociation experiment. Reaction 13 is observed for $NbCH_2^+$, suggesting that

$$NbCH_2^+ + H_2 \rightarrow Nb^+ + CH_4 \quad (13)$$

$D°(Nb^+–CH_2) \leq 112$ kcal/mol. At first glance, reactions 11 and 13 appear inconsistent; however, if $D°(Nb^+–CH_2) \sim 112$ kcal/mol, then either reaction 11 or reaction 13 could be slightly endothermic and might be observed as a slow reaction. However, reaction 13 is rapid compared to reaction 11, implying that reaction 13 is the exothermic channel. $NbCH_2^+$ will react with CH_4 to abstract another carbene, reaction 14,[19] but it does not produce

$$NbCH_2^+ + CH_4 \rightarrow NbC_2H_4^+ + H_2 \quad (14)$$

Nb^+ as a reaction product, which might suggest $D°(Nb^+–CH_2) \geq 96$ kcal/mol. Collision-induced dissociation of $NbCH_2^+$ produces predominantly Nb^+ with some NbC^+ also observed.

$NbCH_2^+$ photodissociates according to reactions 2–4 to generate Nb^+, NbC^+, and $NbCH^+$, all in good abundance. $NbCH^+$, which is the most intense photoproduct, is not observed by collision-induced dissociation of $NbCH_2^+$. Two peaks are observed in the photodissociation spectrum of $NbCH_2^+$, Figure 3a at 240 nm (σ = 0.20 Å^2) and 390 nm.

Figure 3b, the photoappearance spectrum of Nb^+, reveals a threshold at 270 nm, implying $D°(Nb^+–CH_2)$ = 106 ± 7 kcal/mol. This value is somewhat lower than expected from reaction 11, but it is in good agreement with reactions 12 and 13. Increased Ar pressure did not quench dissociation in the 240–260-nm region. On the basis of observation of reaction 11, the photodissociation threshold for Nb^+, and the factors stated above, values of $D°(Nb^+–CH_2)$ = 109 ± 7 kcal/mol and $\Delta H_f°(NbCH_2^+)$ = 316 ± 7 kcal/mol are assigned. For comparison, ab initio calculations indicate that the metal–carbene bond dissociation energy of $H_2(CH_3)NbCH_2$ to the closed-shell singlet fragments $H_2(CH_3)Nb$ and CH_2 is 112 kcal/mol.[6d]

Figure 3c illustrates the photoappearance spectra for $NbCH^+$ and NbC^+. The photoappearance threshold of $NbCH^+$ occurs at 450 nm, indicating $D°(NbCH^+–H)$ = 64 ± 5 kcal/mol. Further calculation provides $\Delta H_f°(NbCH^+)$ = 328 ± 8 kcal/mol and $D°(Nb^+–CH)$ = 145 ± 8 kcal/mol. NbC^+ is observed as a photoproduct at wavelengths at least out to 590 nm, implying $D°(NbC^+–H_2) < 48$ kcal/mol, $\Delta H_f°(NbC^+) < 364$ kcal/mol, and $D°(Nb^+–C) > 138$ kcal/mol. The above values suggest $D°(NbC^+–H) < 88$ kcal/mol. In order to check the value of $D°(Nb^+–C)$, the reaction of Nb^+ with cycloheptatriene was examined. Nb^+ will react with cycloheptatriene to generate a variety of products, including $NbCH_2^+$, but no NbC^+ is observed, possibly implying $D°(Nb^+–C) \leq 148$ kcal/mol.

$D°(Nb–C)$ = 134.8 ± 3.1 kcal/mol has been determined by Knudsen cell mass spectrometry and implies a multiple bond in NbC.[20] Ionization probably does not significantly affect the bond energy, suggesting that a nonbonding electron is removed. IP(NbC) < 6.7 eV is calculated from the bond energies of NbC and NbC^+. PA(NbC) = 247 ± 11 kcal/mol is derived from $D°(Nb–C)$ and $\Delta H_f°(NbCH^+)$.[13]

Bond Energy/Bond Order Relationships

Three structures can be proposed for MCH_2^+, I–III. Structures II and III might be expected to undergo deuterium exchange with

$$M^+—CH_2 \qquad H—M^+—CH \qquad \begin{matrix} H \\ \diagdown \\ M^+—C \\ \diagup \\ H \end{matrix}$$

I II III

C_2D_4, which has been utilized to identify metal–hydride character.[21] However, no deuterium exchange is observed. In addition, the major CID product of MCH_2^+ at high energies is M^+. Structures II and III should produce predominantly MCH^+ and

(15) Jacobson, D. B.; Byrd, G. D.; Freiser, B. S. *Inorg. Chem.* **1984**, *23*, 553.
(16) Shim, I.; Gingerich, K. A. *J. Chem. Phys.* **1984**, *81*, 5937.
(17) Huang, Y.; Wise, M. B.; Jacobson, D. B.; Freiser, B. S. *Organometallics* **1987**, *6*, 346.
(18) Gingerich, K. A.; Pelino, M.; Haque, R. *High Temp. Sci.* **1981**, *14*, 137.
(19) Buckner, S. W.; Freiser, B. S. *J. Am. Chem. Soc.* **1987**, *109*, 1247.
(20) Gupta, S. K.; Gingerich, K. A. *J. Chem. Phys.* **1981**, *74*, 3584.
(21) Jacobson, D. B.; Freiser, B. S. *J. Am. Chem. Soc.* **1985**, *107*, 72.

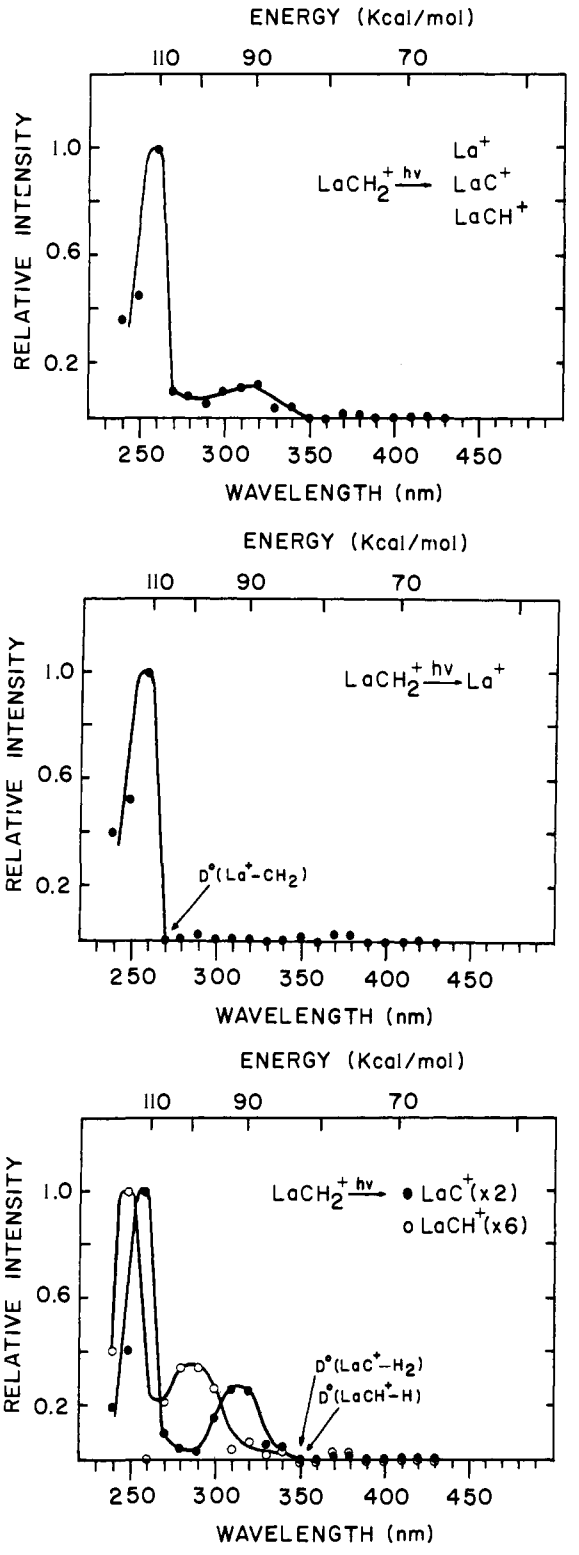

Figure 2. (a, top) The photodissociation spectrum of $LaCH_2^+$ obtained by monitoring all three photoproducts, reactions 2–4, as a function of wavelength. (b, middle) The photoappearance spectrum of La^+ obtained by monitoring reaction 2 as a function of wavelength. (c, bottom) The photoappearance spectra of $LaCH^+$ (open circles) and LaC^+ (closed circles) obtained by monitoring reactions 3 and 4 as a function of wavelength. The intensities of these two photoproducts have been scaled relative to the intensity of La^+ in spectrum b, which was assigned to be 1.0 at 260 nm.

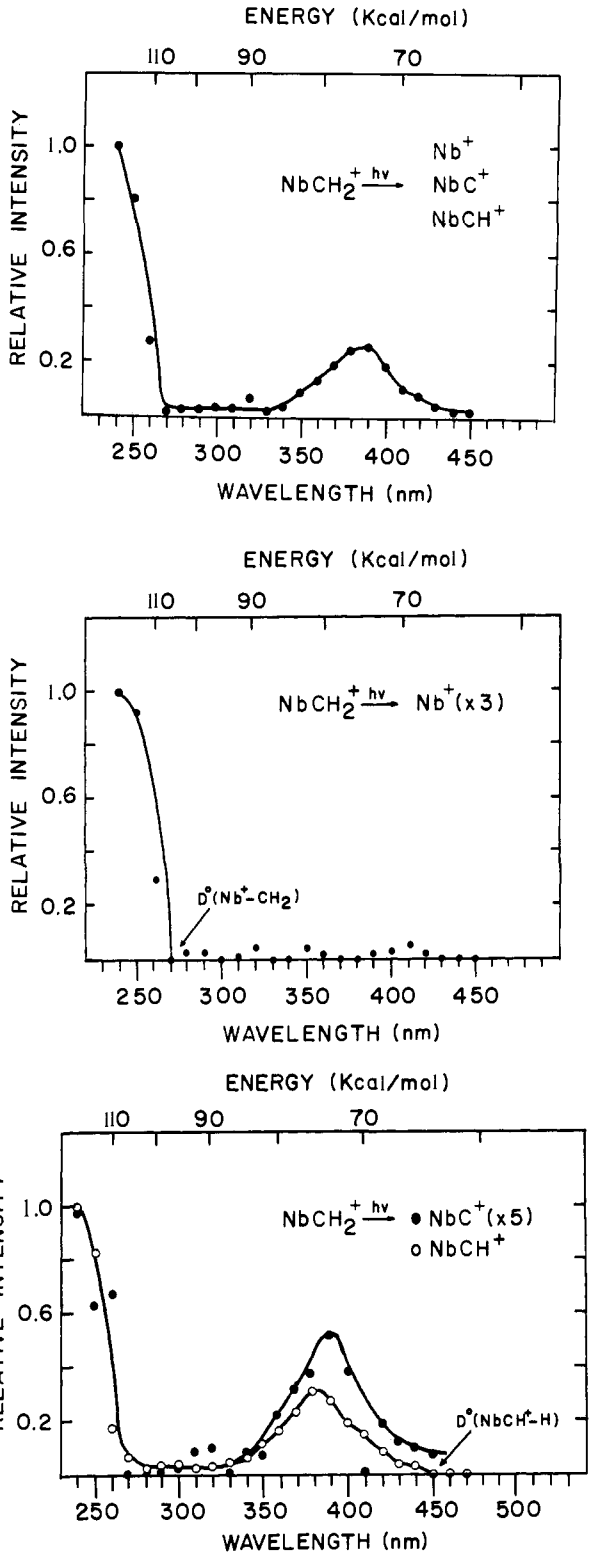

Figure 3. (a, top) The photodissociation spectrum of $NbCH_2^+$ obtained by monitoring all three photoproducts, reactions 2–4, as a function of wavelength. (b, middle) The photoappearance spectrum of Nb^+ obtained by monitoring reaction 2 as a function of wavelength. The intensity of Nb^+ has been scaled relative to the intensity of $NbCH^+$ in spectrum c, which was assigned to be 1.0 at 240 nm. (c, bottom) The photoappearance spectra of $NbCH^+$ (open circles) and NbC^+ (closed circles) obtained by monitoring reactions 3 and 4 as a function of wavelength. The relative intensity of NbC^+ has been scaled to the intensity of $NbCH^+$.

MC^+, respectively, at high energies. $D°(MCH^+-H)$ = 80–90 kcal/mol for M = Fe, Co, Rh, and La is indicative of a C–H bond energy and further suggests structure I. $D°(NbCH^+-H)$ = 64 ± 5 kcal/mol, however, could suggest either structure II or structure III for $NbCH_2^+$, but the CID results of $NbCH_2^+$ (Nb^+ as the predominant fragment at high energies) still favor structure I.

Generally, collision-induced dissociation of MCH_2^+ is different from the photodissociation, with photodissociation always gen-

Table I. Bond Energies for Metal–Ion Ligand Complexes and Hydrocarbons (all values are in kcal/mol)

	$D°(M^+–H)$	$D°(M^+–CH_3)$	$D°(M^+–CH_2)$	$D°(M^+–CH)$	$D°(M^+–C)$	$D°(M^+–O)$	$D°(MCH^+–H)$	$D°(MC^+–H)$
Fe	47.0 ± 4[a]	65 ± 5[b]	82 ± 5[c]	101 ± 7[c]	94 ± 7[c]	68 ± 2[d]	82 ± 5[c]	88 ± 10[c]
Co	45.5 ± 2[a]	57 ± 7[b]	84 ± 5[c]	100 ± 7[c]	90 ± 7[c]	65 ± 2[d]	84 ± 5[c]	91 ± 10[c]
Rh	42 ± 3[e]	47 ± 5[e]	91 ± 5	102 ± 7	164 ± 16[f]	<85[g]	89 ± 5	20 ± 24
La	60 ± 10		106 ± 5	125 ± 8	102 ± 8	205[h]	82 ± 7	104 ± 11
Nb	53 ± 3[a]		109 ± 7	145 ± 8	>138	151 < x < 257[i]	64 ± 5	<88

$D°(H_nC–L)$[j]		$D°(H_nC–L)$[j]		$D°(H_nC–L)$[j]	
$H_3C–H$	104	C–C	145	HC–CH	230
$H_3C–CH_3$	90	$H_2C–CH_2$	173	C–O	257
$H_3C–OH$	91	$H_2C–O$	181		

[a] Reference 25b. [b] Reference 3b. [c] Reference 4. [d] Reference 23. [e] Reference 25a. [f] Reference 15. [g] Reference 12. [h] Reference 29. [i] References 19 and 29. [j] Reference 13.

erating more fragment ions. The reason for this difference, which may be due to the way the energy is added to the ion (e.g., vibrational vs. electronic, stepwise vs. instantaneous), is uncertain at this time.[3,22] Interestingly, when $M^+–C$ is strong (>130 kcal/mol, as for M = Nb, Rh) then MC^+ is observed as a product in the collision-induced dissociation experiment. For M = Fe, Co, and La, no MC^+ is observed in the CID experiment.

One speculative but interesting method of investigating bond energy/bond order relationships, reported by Aristov and Armentrout,[14] has been to plot the bond energies of metal–ligand ions vs. the bond energies of corresponding carbon analogues. These plots have been found to be linear and may be used to predict bond orders. They provide only estimates, however, and cannot unambiguously yield bond orders since $M^+–L$ bonds may not necessarily show the same linear bond order/bond energy correlation as do hydrocarbon bonds. Figure 4a–c illustrates plots for Fe^+, Co^+, Rh^+, Nb^+, and La^+ based on the values given in Table I. Single bond regions are identified by $M^+–H$ bonds whereas all $M^+–CH_2$ bonds examined here are assigned to be double bonds.[23] The origin (0,0) was also used in determining the slope of the line.

Figure 4a shows plots for Fe^+ and Co^+ based on the bond energies for $M^+–H$, $M^+–CH_3$, and $M^+–CH_2$. When the values given above are used, the plot for Fe^+ has a slope of 0.47 and a correlation of 0.94, and the plot for Co^+ has a slope of 0.48 and a correlation of 0.97. For M = Fe and Co, $D°(M^+–C)$ correlates well with $D°(H_2C{=}CH_2)$, suggesting that $M^+–C$ is a double bond. The assignment of $M^+–CH$ is difficult since no other triply bonded $M^+–L$ ions are known (to establish the line in the triple bond region). $M^+–CH$, which could be either a double or a triple bond, appears to correlate best with the C–C bond energy of acetylene, suggesting that it may be a triple bond. These results are identical with those determined for the vanadium ion.[14] The single, double, and triple bond regions for Fe and Co are identified at the top of Figure 4a. On the basis of these plots, $D°(M^+–O) \sim 66$ kcal/mol for both iron and cobalt[24] indicates that $M^+–O$ here are single bonds, similar to the C–O bond in alcohols. This is in contrast to early transition metals (Sc, Ti, V) where $M^+–O$ may be a triple bond.[14,24] Apparently the formation of a multiple bond between M^+ and O requires empty $d\pi$ orbitals on the metal which can be filled by back donation of oxygen electron density. FeO^+, CoO^+, and NiO^+, which are predicted to be single bonds based on plots such as Figure 4a, show excellent inverse correlation between $D°(M^+–O)$ and the energy required to promote the metal ion into an s^1d^n electronic configuration,[25] implying that the 4s orbital of the metal is a major component of the $M^+–O$ bond. No such correlation is observed for early transition metal oxides.[24]

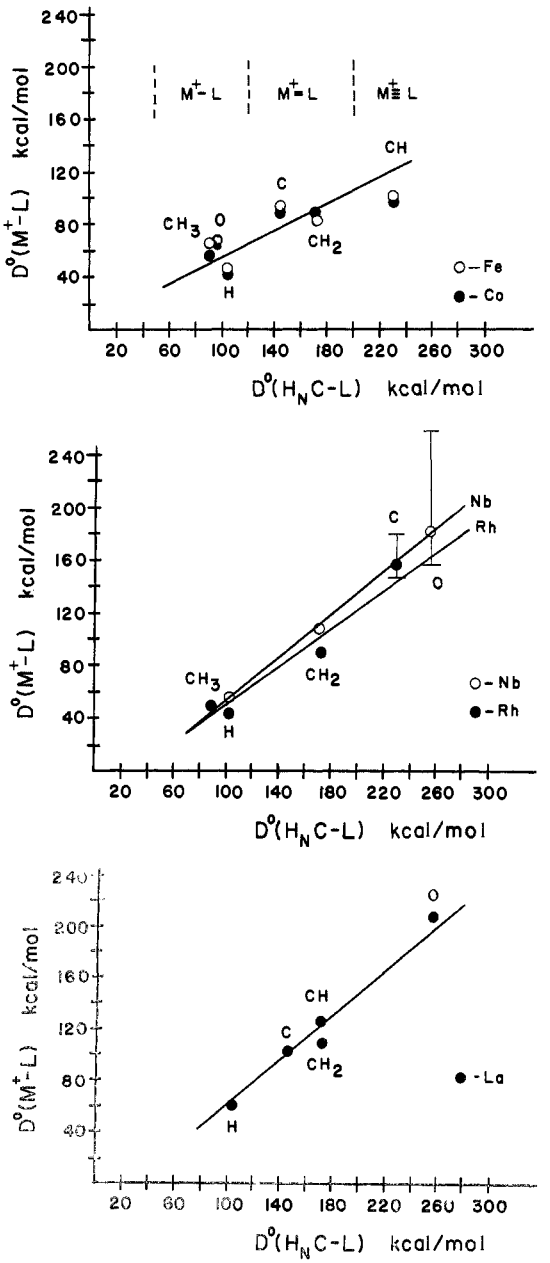

Figure 4. (a, top) Correlation plots of $Fe^+–L$ and $Co^+–L$ bond energies vs. bond energies of corresponding carbon analogues. Values are taken from Table I. Specifically, each line is defined by the origin at $X = 0$, $Y = 0$, the single bond region at $X = D°(CH_3–CH_3) = 90$ kcal/mol, $Y = D°(M^+–CH_3)$, and $X = D°(CH_3–H) = 104$ kcal/mol, $Y = D°(M^+–H)$, and the double bond region at $X = D°(CH_2{=}CH_2) = 173$ kcal/mol, $Y = D°(M^+–CH_2)$. The bond orders for $M^+–C$, $M^+–CH$, and $M^+–O$ are then predicted by their best fit on the line. (b, middle) Correlation plots of $Rh^+–L$ and $Nb^+–L$ bond energies vs. bond energies of corresponding carbon analogues. (c, bottom) Correlation plot of $La^+–L$ bond energies vs. bond energies of corresponding carbon analogues.

(22) Franchetti, V.; Freiser, B. S.; Cooks, R. G. *Org. Mass Spectrom.* **1978**, *13*, 106.

(23) Theoretical calculations (ref 6a and 6b) and experimental studies (Armentrout, P. B.; Halle, L. F.; Beauchamp, J. L. *J. Am. Chem. Soc.* **1981**, *103*, 6501) indicate that the bond for $M^+–CH_2$ where M is a transition metal is a double bond.

(24) Armentrout, P. B.; Halle, L. F.; Beauchamp, J. L. *J. Am. Chem. Soc.* **1981**, *103*, 6501.

(25) For a discusslon of the promotion energy/bond order relationship, see: (a) Mandich, M. L.; Halle, L. F.; Beauchamp, J. L. *J. Am. Chem. Soc.* **1984**, *106*, 4403. (b) Elkind, J. L.; Armentrout, P. B. *Inorg. Chem.* **1986**, *25*, 1078.

The high value of $D°(Rh^+–C)$ is much greater than $D°(Rh^+–CH_2)$, which is postulated to be a double bond. Indeed, correlation of $D°(Rh^+–C)$ with $D°(HC{\equiv}CH)$ in the plot in Figure 4b suggests that $Rh^+–C$ may have a triple bond. Interestingly, $Co^+–C$ was postulated to be a double bond. Since both Rh^+ and Co^+ have identical ground states (d^8, $^3F_4$),[26] apparently the larger ionic size of Rh^+ facilitates multiple bonding.

Assuming the single, double, and triple bond regions for Rh^+ are defined by $Rh^+–H$, $Rh^+–CH_2$, and $Rh^+–C$, respectively, yields a line with a slope of 0.63 and a correlation of 0.98, Figure 4b. On the basis of this line, $Rh^+–CH$ is obviously not a triple bond (i.e., $D°(Rh^+–CH)$ = 102 kcal/mol does not correlate with $D°(HC{\equiv}CH)$ = 230 kcal/mol). This point has been left off Figure 4b for clarity. This result and $D°(RhC^+–H) = 20 \pm 24$ kcal/mol[27] might imply that the correct structure of $Rh^+–CH$ is structure IV, which is reasonable considering the strong $Rh^+–C$

$$\underset{\text{IV}}{H–Rh^+{\equiv}C}$$

bond. Unfortunately, the intensity of $RhCH^+$ was too low to permit isolation and reaction with C_2D_4 to investigate H/D exchange. $Rh^+–O$ has been predicted to be a weak bond.[28] Indeed, absence of formation of RhO^+ from reaction 5 might imply $D°(Rh^+–O) < 85$ kcal/mol (this is the energy required to abstract oxygen from ethylene oxide[13]). Plotting this upper limit on Figure 4b suggests that $Rh^+–O$ is probably a single bond, in analogy to $Co^+–O$. As mentioned earlier, empty d orbitals, which appear to be required to form a multiple bond between M^+ and O, are not present on either Rh^+ or Co^+.

$RhCH_3^+$ has been predicted to exist as structure V rather than structure VI,[12b] based on the fact that $D°(RhCH_2^+–H) = 62 \pm$

$$\underset{\text{V}}{H–Rh^+–CH_2} \qquad \underset{\text{VI}}{Rh^+–CH_3}$$

10 kcal/mol is nearer to $D°(Rh^+–H) = 42 \pm 5$ kcal/mol[25a] than $D°(CH_2–H)$ = 109 kcal/mol.[13] $D°(Rh^+–CH_2) = 91 \pm 5$ kcal/mol determined in this study and $D°(Rh^+–CH_3) = 47 \pm 5$ kcal/mol[25a] yield $D°(RhCH_2^+–H) = 65 \pm 5$ kcal/mol. This value coincides somewhat more closely with the C–H bond energies of reactions 15 and 16,[13] which are examples where the CH_2 can

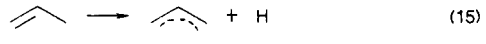

$$\Delta H° = 88 \text{ kcal/mol} \qquad (15)$$

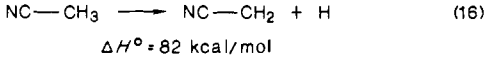

$$\Delta H° = 82 \text{ kcal/mol} \qquad (16)$$

be stabilized by multiple-bond formation, as would be the case for $Rh^+–CH_2$. This suggests that $Rh^+–CH_3$ as a single bond structure VI is possible. Indeed, Figure 4b indicates that $Rh^+–CH_3$ fits well into the single bond region defined by $Rh^+–H$.

$Nb^+–O$, which would be predicted to be a triple bond (similar to $V^+–O$), has a bond energy which has been bracketed between 151 and 257 kcal/mol.[19,29] Single, double, and triple bond regions for Nb^+ can be defined by $Nb^+–H$, $Nb^+–CH_2$, and $Nb^+–O$ as shown in Figure 4b, producing a line with slope of ~0.70. The structure of $Nb^+–CH$ is difficult to predict since only an upper limit could be obtained for $D°(NbC^+–H) < 88$ kcal/mol. However, placement of $Nb^+–CH$ ($D°(Nb^+–CH)$ = 145 kcal/mol) in Figure 4b suggests that it may be a triple bond, correlating with $HC{\equiv}CH$. $D°(Nb^+–C) > 138$ kcal/mol implies that $Nb^+–C$ is also a triple bond, in contrast to $V^+–C$, which was predicted to be a double bond.[14] Both Nb^+ and V^+ have the same ground state (d^4, $^5D_0$) with a relatively low-lying (~2500 cm^{-1}) d^3s^1 state,[26] so again ionic size might be the dominant factor.

$La^+–O$ is estimated to be a triple bond, similar to $Sc^+–O$, and has a bond energy of 205 kcal/mol.[30] $D°(La^+–H)$ can be assumed to be approximately 60 ± 10 kcal/mol.[31] Assuming then that $La^+–H$, $La^+–CH_2$, and $La^+–O$ define the single, double, and triple bond regions, respectively, Figure 4c indicates a line with a slope of 0.78 and a correlation of 0.98. On this scale, $La^+–C$ is predicted to be a double bond. $D°(LaC^+–H) = 104 \pm 11$ kcal/mol indicates that $LaCH^+$ exists as $La^+–CH$ and not $H–La^+–C$. Interestingly, Figure 4c predicts that $La^+–CH$ is also a double bond. This is reasonable since La^+ has only two unpaired electrons (d^2, $^3F_2$ ground state)[26] and cannot combine with three unpaired carbon electrons to produce a triple bond. For a strong $M^+–C$ or $M^+–CH$ bond to form, M^+ must have a suitable number of unpaired electrons which can combine with the unpaired carbon electrons to form the multiple bond.

One interesting aspect of these plots is that, in general, there appears to be a roughly linear correlation between the sizes of the metal ions and the slopes of the lines from plots such as Figure 4. This result may imply that large metal ions form stronger double and triple bonds with ligands than do small metal ions.

Acknowledgment is made to the Division of Chemical Sciences in the Office of Basic Energy Sciences in the United States Department of Energy (DE-AC02-80ER10689) for supporting the transition metal ion research and to the National Science Foundation (CHE-8310039) for continued support of the Fourier transform mass spectrometry instrumentation. R.L.H. gratefully acknowledges the W.R. Grace Company for providing fellowship support.

Registry No. $RhCH_2^+$, 98194-45-7; $NbCH_2^+$, 106681-94-1; $LaCH_2^+$, 105039-61-0.

(26) Moore, C. E. *Natl. Stand. Ref. Dat. Sec., Natl. Bur. Stand.* **1971**, *2–3*.

(27) This value was calculated with $D°(Rh^+–CH) = 102 \pm 7$ kcal/mol and $D°(Rh^+–C) = 164 \pm 16$ kcal/mol (ref 15).

(28) Byrd, G. D. Ph.D. Thesis, Purdue University, 1982.

(29) Kappes, M. M.; Staley, R. H. *J. Phys. Chem.* **1981**, *85*, 942.

(30) Murad, E.; Hildenbrand, D. L. *J. Chem. Phys.* **1980**, *73*, 4005.

(31) Experimental investigations of the first and second row transition metal–ion hydrides (ref 25b) indicate that the maximum metal hydride bond energy is probably ~60 kcal/mol. La^+ exists as s^1d^1 in the ground state (ref 26), so $D°(La^+–H)$ should be very near the maximum bond energy value (similar to $D°(Y^+–H) = 58 \pm 3$ kcal/mol, ref 25b).